CHAPTER

22

Reconstitution of membrane symmetry breaking

Shiva Razavi[1,2] *and Takanari Inoue*[1,2]

[1]Department of Biomedical Engineering, Johns Hopkins University School of Medicine, Baltimore, MD, United States [2]Department of Cell Biology, Center for Cell Dynamics, Johns Hopkins University School of Medicine, Baltimore, MD, United States

Symmetry, as wide or as narrow as you define its meaning is one idea by which man through the ages has tried to comprehend and create order, beauty, and perfection. ***Hermann Weyl*** *(Weyl, 1952)*

22.1 Introduction

Our understanding of nature is often punctuated by consideration of symmetry. Natural processes are continuously transitioning between evolving structures that serve unique functions. Identifying the molecular interactions that dictate the trajectories between these symmetry states is an overarching theme in biology. As biological systems operate via entangled, redundant, and spatially-regulated molecular interactions, the stepwise determination of these transition states is impossible. Therefore, a macroscopic view of symmetry in a biologically reduced context makes such studies more tractable. Symmetry breaking events such as vesicular trafficking, cell division, or cell migration dynamically translate molecular interactions into events that perturb the membrane boundary. Therefore, to assess symmetry, the reduced biological context should be able to capture the cell's lipid membranes. Here, we present an overview of how closed, cell mimetic membranes could be adopted to engineer systems that can depart from symmetries toward asymmetric architectures. This sharpens the reader's understanding of the governing principles of symmetry breaking and inspires insights into how dynamic reorganization events drive key functions of a living cell.

Plasma Membrane Shaping
DOI: https://doi.org/10.1016/B978-0-323-89911-6.00027-3

For cells to divide, move, ingest, communicate, and differentiate, biomolecules reorganize and signal on the membrane to ultimately change the architecture of the cell boundary and break symmetry. In all these processes, the biomolecular composition of the cell remains unchanged while its geometry evolves between a plethora of unique morphologies (Fig. 22.1A and B). As Helfrich postulated, the chemical reactions taking place inside a membrane-bound compartment can alter the elastic stiffness of the boundary and break its symmetry (Helfrich, 1973). Given a particular output function (i.e., fusion, fission, endocytosis, exocytosis, or movement), we present a series of works that through reconstitution efforts have identified biochemical reactions that can trigger a desired membrane morphogenesis event. Here, we direct our focus to membrane systems that permit observation of morphologies via standard microcopy techniques.

We survey a body of research efforts where different *in vitro* model membrane systems such as giant unilamellar vesicles (GUVs), large unilamellar vesicles (LUVs), small unilamellar vesicles (SUVs), and supported lipid bilayers (SLBs) were used to probe biochemical reactions in the context of symmetry breaking (Fig. 22.1C). We first present a few studies where membrane detachment or attachment were achieved, highlighting several key regulatory modes (Fig. 22.1). We then present movement in the context of adhesion-dependent cell motility where the polarization of the plasma membrane in the form of a leading edge and a trailing

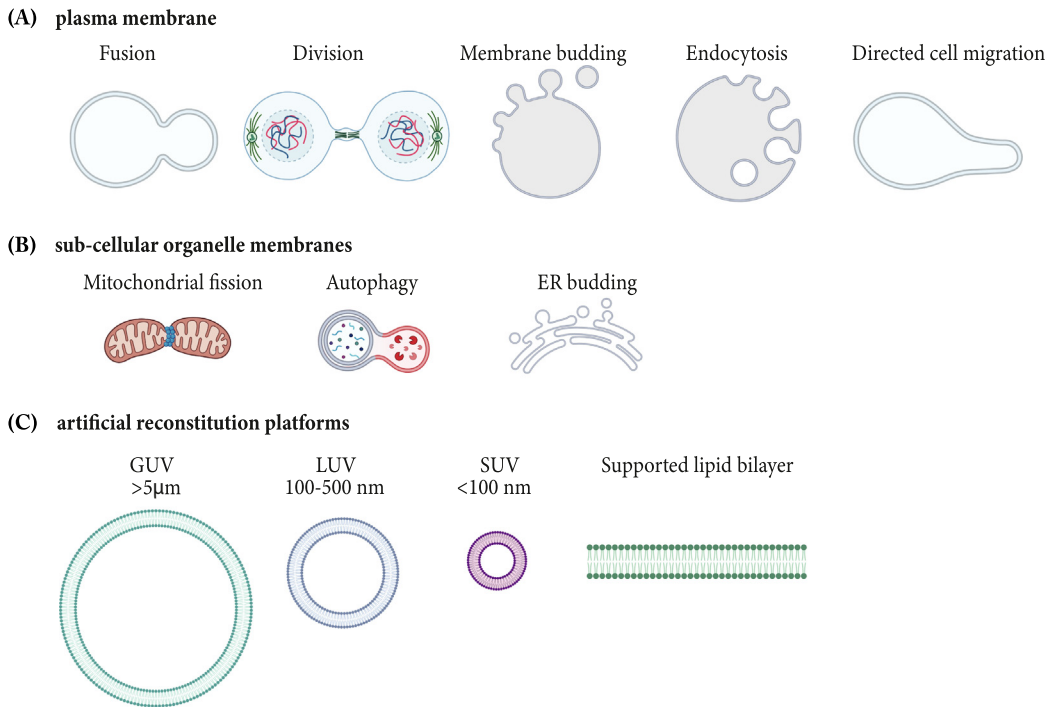

FIGURE 22.1 Cell biological events that rely on symmetry breaking to achieve an output on (A) a cellular level or (B) subcellular level. (C) Representative reconstitution platforms to study biomolecular interactions in the context of biological membranes.

rear needs to be achieved. Finally, we conclude that to build self-sufficient synthetic cells, membranous bioreactors that can autonomously synthesize the precursor biomolecules or energy need to be realized. These efforts not only enable identifying the minimal molecular components that drive complex cell functions, but could be used to test *de novo* biochemical processes. Moreover, with the knowledge of the physical principles garnered, we can engineer autonomous, biohybrid systems for applications in medicine and biotechnology. Collectively, these efforts are foundational steps that enable building a molecular map of how cells function and ultimately aid in devising the next generation of micron-sized machines.

22.2 Membrane fusion, fission, and trafficking

The ability of cells to divide and reproduce sustains life. Cells undergoing division polarize their membrane in the form of dumbbell structures that ultimately morph into two distinctly detached daughter cells. Similarly, for vesicular trafficking and endocytosis, membranes need to separate. It is known that drastic increase in the spontaneous curvature of the membrane followed by an ATPase/GTPase driven membrane pinching detaches cells or vesicles from each other. Mechanisms implicated in formation of spontaneous membrane curvature include: (1) membrane scaffolding by proteins or complexes that are structurally curved, such as clathrin, Bin/Amphiphysin/Rvs (BAR) domains, (2) insertion of amphipathic helices such as tubulin, epsin1, Sar1p, Arf1, and M2 influenza proteins, (3) nonstructural modulators including protein-protein interaction, or (4) liquid-like protein interactions on the membrane. Cells use a combination of these strategies in concert to achieve fission. To discern how each of these processes modulate division we overview a subseries of reconstruction efforts that have provided key insight.

22.2.1 Structurally curved elements in bacteria

To explore morphogenesis, it is pertinent to consider the cells' initial morphologies and locate the molecules that contribute to these basal structures. For bacteria to maximize their surface area to volume ratio, they assume an elongated shape. This rod-like morphology is mostly attributed to the MreB protein that is a bacterial analog of actin. Previously the cell-free *in vitro* transcription-translation system (IVTT) was used to express MreB and MreC together with the membrane pore-forming α-hemolysin protein that allows $Mg^{2+}$and ATP uptake to trigger cytoskeletal assembly inside a giant vesicle. While filamentous structures formed on the membrane, no drastic deformation was observed (Maeda et al., 2012). However, when PEG as a crowding agent and IVTT-synthesized MreB protein were encapsulated in giant vesicles, the cytoskeletal structure that emanated was potent enough to deform the vesicles smaller than 10 μm in diameter (Garenne et al., 2020) (Table 22.1, Fig. 22.2 – No. 1). This dimension matches that of bacteria that is typically 0.5–10 μm in length and 0.25–1 μm in diameter. Given the molecular crowding can affect both the osmolarity and the membrane properties, a synergetic assessment of the protein modules and membrane considerations (e.g., mechanical and phase separation properties) is integral to reconstituting membrane biology.

TABLE 22.1 Representative studies on the use of membrane-mimetic platforms to reconstitute molecular organization, shape morphogenesis, and material (e.g., ATP, lipid, and oligonucleotide) synthesis.

No.	Biological context	Spadai context	Reconstiuted membranes	Key proteins/buffer modules	Output pattern/ function	References
1	Bacterial shape	Inside GUV	PC:PE-PEG5000 (99:0.66 mol%)	MreB [>10 μM]	Rod-like structure in vesicles	Garenne et al. (2020)
2	Endocytosis	On GUV/Mica supported bilayer	Brain sphingolipids: DOPS: PIP_2 (60:30:10 mol%) with 50% cholesterol	Clathrin [0.4 μM], AP180 [0.5 μM], epsin	Budding	Saleem et al. (2015)
3	Membrane fission	Microbeads-supported bilayer with excess lipid reservoir (SUPER)	DOPC:DOPS:PI-4,5:RhPE (79:15:5:1 mol%)	Dynamin [0.5 μM], GTP [1 mM]	Membrane tubulation, budding, and puncta structures	Pucadyil and Schmid (2008)
4	Cell division, cytokinesis, and viral budding	Outside GUV	POPC:POPS:cholesterol:PtdIns(3) (62:10:25:3 mol%)	Snf7 [600 nM], Vps24 [200 nM], Vps2 [200 nM], Vps4 [200 nM]	Vesicularization and uptake by GUV	Wollert et al. (2009)
5	Cell division, cytokinesis, and viral budding	Inside GUV	POPC:POPS:PS (79.1: 20.5: 0.2 mol%)	Snf7 [2 μM], Vps2 [2 μM], Vps4 [2.6 μM], caged ATP [2 mM]	Pulled nanotubes triggered protein-induced forces and scission	Schöneberg et al. (2018)
6	Bacterial division	Planar supported lipid bilayer	*E. coli* lipid extracts and 0.1 mol% DiIC-C18	MinD [1 μM], MinE [1 μM], ATP [2.5 mM]	Spiral waves	Loose et al. (2008)
7	Bacterial division	Inside GUV	DOPC:DOPG (4:1 mol%)	MinD [1.5 μM], eGFP-MinD [1.4 μM], MinE [3 μM], ATP [5 mM]	Pole-to-pole oscillation, periodic dumbbell splitting and budding	Litschel et al. (2018)
8	Bacterial division	Outside to Inside LUV	DOPG:Egg-PC (2-40:up to 100 mol%)	membrane targeted-FtsZ [4 μM], GTP [400 μM]	FtsZ relocalization from outside to inside of vesicles and Z-ring formation	Osawa et al. (2008)
9	Bacterial division	Supported lipid bilayer and inside SUV	DOPC:DOPG:DGS-NTA (4:1:0.25 mol%)	FtsZ [3 μM], FtsA [∼2.4 μM], ZapA [∼ 0.4 μM], GTP [2 mM], ATP [2 mM]	Formation of filament network on SLB, budding and force generation in GUVs	Godino et al. (2020)

10	Cell division	Outside GUV	POPC:POPG: cholesterol (70:10:20 mol%)	His-tagged GFP [15.6-39 nM]	Dumbell, necking, and fission	Steinkühler et al. (2020)
11	Autophagy	Outside LUV and GUV	POPC:POPE:liver PI:DPPE-PEG2000 (59:30:10:1 mol%)	Atg8 [100 μM], Ag19WT -[1 μM], Ape1WT [20 μM]	Sequestration of Apel condensate by precursor membranes	Yamasaki et al. (2020)
12	Autophagy	Outside GUV	PC:PE:DOPS:PI(3)P (72.8:20:5:2:0.2 mol%)	PISKC3-C1 [0.1 μM], WIPI2d [0.25 μM], E3-GFP [0.1 μM], ATG7 [0.1μM], ATG3 [0.1 μM]	Lipidation	Fracchiolla et al. (2020)
13	Cytoskeletal reorganization	Inside GUV	Egg-PC:DOPS:DOPE-biotin (75:25:0.05 mol%)	Centrosome, tubulin [15-40 μM], GTP	Deformation with elongated asters	Gavriljuk et al. (2021)
14	Motility and division	Inside GUV	DOPC:DPPC:cholesterol:DSPE-PEG2000 (4:4:1.9:0.1 mol%)	DNA, microtubule, kinesin	Dynamic membrane deformation	Sato et al. (2017)
15	Motility and division	Inside GUV	DOPC	Self-phoretic Janus polystyrene particles	Membrane deformation	Vutukuri et al. (2020)
16	Motility and division	Inside nematic vesicles	Egg-PC:PEG2000PE (95:5 mol%)	Microtubules, kinesin motor, ATP	Morphogenesis with oscillatory dynamics	Keber et al. (2014)
17	Motility and division	Inside GUV	PC:PE (1:4 mol%)	Actin [48 μM], gelsolin [24 nM], ATP [0.2 mM]	Membrane deformation	Cortese et al. (1989)
18	Motility and division	Inside GUV	DMPC:cardiolipin (1:1 wt%)	Actin [100 μM], rhodamine-conjugated phalloidin, ATP [0.2 mM]	Dumbbell shape structures	Miyata and Hotani (1992)
19	Motility and division	Inside GUV	DOPC	F-actin [76 μM], gelsolin [760 nM]	Reversible shape change in response to light irradiation of actin	Tanaka et al. (2018)
20	Motility	Inside GUV	DOPC:PEG-PE: biotein-PE (95.5:2.5:2 mol%)	G-actin [12 μM] , fascin [0.6-2.4 μM]	Actin-web and protrusion on the membrane	Tsai and Koenderink (2015)
21	Material synthesis	Outside GPMV	Extracted RPE cell membrane	GFP-FUC LC [2 μM]	Inward tubulation and pearling of the membrane	Yuan et al. (2021)

(*Continued*)

TABLE 22.1 (Continued)

No.	Biological context	Spadai context	Reconstiuted membranes	Key proteins/buffer modules	Output pattern/ function	References
22	Synthesis and motility	Inside small unilamellar vesicle and GUV	SUV:POPC::POPE:POPG: cholesterol, (2:1:1:1mol%) and GUV: DOPC: POPE:DOPS: cholesterol:PEG2000-PE (2:1:2:1:1 mol%)	ATP synthase, photosystem II, proteorhodopsin, ADP [5 mM], G-actin	ATP synthetis that drove actin polymerization, deforming the memrbane	Lee et al. (2018)
23	Growth and division	Multilamellar vesicles and micelles	Oleate (C18:l) fatty acid	Oleate micelles, RNA	Vesicle growth and division induced by external shear forces	Zhu and Szostak (2009)
24	DNA amplification and division (reproduction)	Inside GUV	POPC:POPG:cationic membrane molecules: acidic catalyst (6:2:2:1 mol%)	PCR reaction (DNA, polymerase, dNTP, Mg^{2+}, ATP)	DNA amplification and division	Kurihara et al. (2011)
25	Growth and division	Inside LUVand GUV	DOPC:DOPE:DOPG:cardiolipin: DHPE-Texas Red:DSPE-PEG-biotin (50:36:12:2:0.5:1 mol%)	DNA encoding *plsB*, *plsC*, *cdsA*, *pgsA*, *pgpA*, *pssA*, and *psd*	Synthesis of DOPE, DOPG, DPPE, DPPG, POPE, and POPG lipids	Blanken et al. (2020)

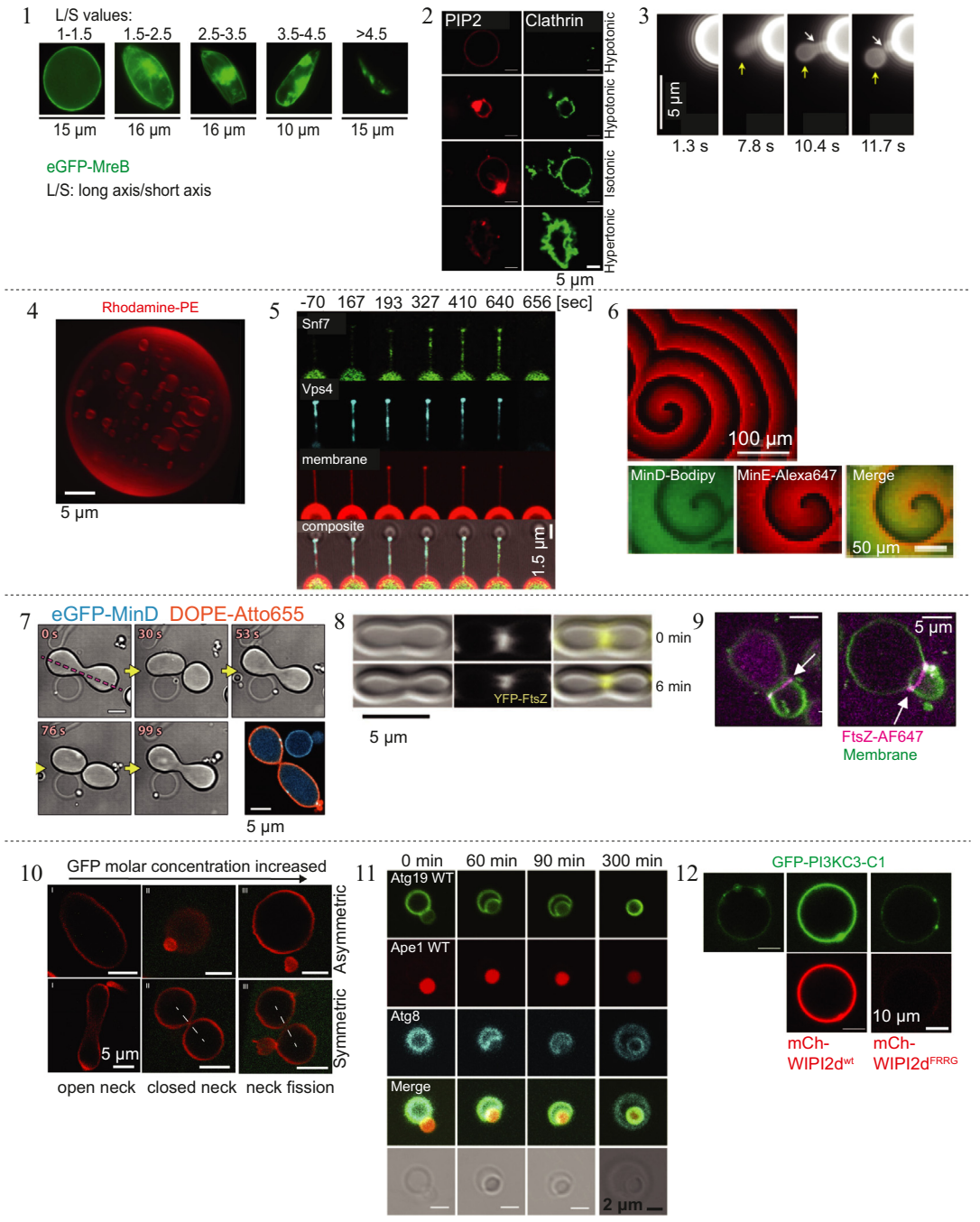

FIGURE 22.2 Representative images of the platforms presented in Table 22.1 (Nos. 1–12). Images are reprinted from the cited sources, either with permission of the respective copyright holders or under a Creative Commons license.

22.2.2 Structurally curved elements in eukaryotes

Although it is well known that assembly of triskelion, the basic structural unit of a clathrin lattice, drives the budding of spherical vesicles essential for membrane trafficking, it is unclear exactly how clathrin reorganizes the membrane morphology. Clathrin's association with the membranes is achieved by protein adapters including AP180 or epsin 1 that binds clathrin both directly and via the AP-2 adapter complex (Drake et al., 2000). Epsin contains an amphipathic helix that wedges itself into the membrane and enables curvature generation. To assess if the elasticity of the membrane regulates the assembly and shape of clathrin lattices, GUVs mimicking the composition of the inner leaflet of the plasma membranes were placed in buffers of different osmolarity containing clathrin and the AP180 adapter. As no membrane deformation was observed with 0.5 μM AP180, protein crowding had negligible effect on deformation. In addition, AP180 and clathrin deformed the membrane at high membrane tensions. However, when epsin was added, the membrane deformation properties favored polymerization of clathrin irrespective of membrane tension (Saleem et al., 2015) (Table 22.1, Fig. 22.2 – No. 2). These reports collectively highlight that the roles of membrane wedging, crowding, and scaffolding are synergistic and cannot be easily parsed.

Dynamin GTPase is strongly implicated in clathrin-dependent endocytosis and vesicular trafficking. This molecular scissor acts on a number of different cellular membranes to regulate diverse processes including endocytosis, organelle fission and fusion, synaptic transmission, and muscle contraction. Dynamin GTP hydrolysis rapidly displaces dynamin from the membrane surface. Due to this fast membrane binding and dissociation kinetics (Morlot & Roux, 2013), it is in general challenging to experimentally interrogate its mechanism of action inside living cells. Purified dynamin has a spiral structure and can polymerize on the membrane to form helical tubes. Earlier models described that these preassembled dynamin spirals drive fission in the presence of GTP. Leveraging the SLB with excess membrane reservoir (SUPER) platform, however, revealed that preassembled dynamin supplemented with GTP did not promote fission but dissociated due to its disassembly. In contrast, fission occurred once dynamin was added to SUPER in a constant supply of GTP, highlighting that dynamin assembly itself drives fission (Pucadyil & Schmid, 2008) (Table 22.1, Fig. 22.2 – No. 3). Taken together, distinct outputs could be achieved depending on the "assembly state" of the dynamin input.

For vesicular trafficking in the context of viral budding, host cell membranes must protrude and break. Endosomal sorting complexes required for transport (ESCRT) machinery is established as a key modulator of these processes. ESCRT-III consisting of Vps20, Snf7, Vps24, Vps2 (also known as Did4) assembly is fueled with Vps4 ATPase and ATP. Reconstitution of the purified ESCRT modulators outside GUVs revealed that Vps20, Snf7, and Vps24 are sufficient for uptake of budding vesicles by the GUV. Addition of Vps4 that is recruited to the membrane via Vps2 and Vps24 supports recycling and rounds of budding (Wollert et al., 2009) (Table 22.1, Fig. 22.2 – No. 4). Alternatively, Snf7, Vps24, Vps2, and ATP were reconstituted inside the GUVs, and the membrane was pulled with an optical tweezer to create high membrane curvature regions. This revealed that Snf7 has curvature sensing properties and above a curvature threshold can generate force and ultimately detach the membrane (Schöneberg et al., 2018) (Table 22.1, Fig. 22.2 – No. 5).

Sequential polymerization of ESCRT-III driven by the Vps4 ATPase culminated in formation of helical filaments that deformed the membrane and once formed copolymers with Did2 and Ist1 promoted fission (Pfitzner et al., 2020). This underlines the fact that the signaling output is not merely a function of the identity of biomolecular interactions, and the sequence of these interactions could also be determinant in symmetry breaking.

22.2.3 Positioning of the structural elements

How the structural protein elements organize on the cell membrane determines the deformation output observed. Therefore, the modulators of this positioning illuminate membrane shape morphogenesis.

For bacteria to divide, they first elongate and through the guidance of a Z-ring that defines the mid-cell, the septum separates the two daughter cells by pinching the membrane. How do cells determine the location of the mid-cell? The bacterial Min family of proteins, MinC, MinD, and MinE are known to operate in concert to define the division site. MinD that is initially homogenously distributed on a 2D membrane surface developed into dynamic waves upon addition of MinE and ATP-containing buffer. The nodes of the waves marked regions devoid of either of the two proteins, highlighting Min's temporal modulation of patterning (Loose et al., 2008) (Table 22.1, Fig. 22.2 – No. 6). Translating this reaction to the 3D space of GUVs featured a similar oscillatory membrane shape morphogenesis. While with microscopic assessment, GUVs approximated a seemingly near perfect sphere, the extreme reorganization events in this case achieved periodic membrane budding and splitting of GUVs that morphed into dumbbell shapes (Litschel et al., 2018) (Table 22.1, Fig. 22.2 – No. 7). Therefore, these minimal approaches revealed that perhaps the Min family of proteins' role is far beyond a pointer to the division location. Indeed, recently it was reported that the MinDE protein system can play a role in active transport. MinDE self-organization exerted an effective frictional force on a membrane-bound DNA origami cargo resulting in its directional diffusiophoretic transport (Ramm et al., 2021). Although this mode of dispersed particle motion has been previously well-studied in soft matter physics and chemical physics, this is the first report of such mechanism in a biological context.

FtsZ, a tubulin homolog, is a key cytoskeletal protein that orchestrates the assembly of Z-ring at mid-cell. Reconstitution of an engineered membrane-bound FtsZ inside LUVs revealed that FtsZ alone can generate the constriction forces necessary for Z-ring formation (Osawa et al., 2008) (Table 22.1, Fig. 22.2 – No. 8). However, FtsZ's contributions to division is still a topic of debate (Daley et al., 2016; Söderström et al., 2014). It is postulated that a complete scission requires FtsA protein that recruits FtsZ and auxiliary proteins to the membrane (Osawa & Erickson, 2013). When FtsZ and FtsA were reconstituted on a SLB they formed dynamic ring-like patterns whereas inside GUVs the polymerization reaction deformed vesicles smaller than 15 μm in diameter. ZapA protein that stabilizes and stiffens the FtsZ filament or Ficoll70 crowding agent could each alter the observed 2D morphologies (Godino et al., 2020) (Table 22.1, Fig. 22.2 – No. 9). FtsZ, FtsA, and membrane targeted ZipA only deformed the membrane (Furusato et al., 2018). Reconstitution of the FtsZ, FtsA, and ZapA modules in the GUVs created budding and long membrane

neck formation but not scission (Godino et al., 2020). These highlight that colocalization of FtsZ and FtsA alone does not support fission, and to transition from deformation to neck formation, the FtsZ stiffness had to be modulated. FtsZ protein tethered in the inner GUV membrane could deform the vesicle and create membrane buds via torsional stresses depending on the GTPase activity (Ramirez-Diaz et al., 2021). The field is now actively moving toward interfacing these bottom-up systems with more complexity by considering proteins such as ZapB, FzlC, and SlmA (Cabré et al., 2015; Meier et al., 2016; Monterroso et al., 2019) that could potentially aid in achieving unambiguous fission *in vitro*.

22.2.4 Nonstructural elements

Molecular crowding: Can any inducer of spontaneous membrane curvature promote fission? Steric forces that arise from protein crowding on the membrane are indeed effective in spontaneously curving membranes and promoting division (Stachowiak Jeanne et al., 2010). Notably, epsin 1 in the clathrin mediated endocytic pathway could drive membrane curvature even in the absence of its amphipathic helix (Stachowiak et al., 2012). Similarly, amphipathic helix mutant form of epsin 1 was equally efficient in increasing the spontaneous membrane curvature to promote fission in LUVs. In this system, even molecular crowding achieved by 20 μM green fluorescent protein (GFP) tethered to the DGS-NTA(Ni) containing membrane via a hexa-histidine-tagging (6xHis-GFP) effectively drove membrane curvature, likely via a steric effect (Snead et al., 2017). However, more dilute His-tagged GFP (~15 nM) or His-tagged improved light-induced dimer module (His-iLID) outside either 200 nm LUVs or 20 μm GUVs made with 0.1 mol% NTA-conjugated lipids could also divide the vesicles (Steinkühler et al., 2020) (Table 22.1, Fig. 22.2 – No. 10). Moreover, in this work the average distance between membrane anchored GFPs was reported as larger than 24 nm, exceeding the GFP's lateral size of 3 nm. Therefore, the observed division is considered independent of the steric interactions between the GFP molecules. These observations highlight that the protein concentration rather than the identity of the molecular interactions themselves drive the spontaneous membrane curvature forces. It is notable that the forces generated compared well with the ones implemented by dedicated protein complexes in the division signaling pathways. These protein-based approaches in engineering division are well-suited as simpler design modules for the synthetic biology community that aims at engineering an output rather than achieving a perfect mimicry of the cell.

22.3 Autophagy

Intracellular waste products need to be packaged in unique membrane structures that are delivered to lysosomes for degradation and recycling. This process, known as autophagy, requires the formation of membrane precursors that can encapsulate the cytosolic cargo. For cells to maintain their homeostasis, autophagy as a housekeeping mechanism removes a cell's misfolded or aggregated proteins and dysfunctional components to balance its energy sources. Autophagy could be selective or nonselective with its target. Some condensates that are formed through liquid-liquid phase separations (LLPS) of biomolecules such as nucleic acids

and proteins are cleared via selective autophagy. Precursor isolation membrane (IM) engulfs condensates leading to formation of membrane-bound autophagosomes that are destined for degradation via fusion with lysosome. Selective autophagic cargo aminopeptidase I (Ape1) that undergoes phase separation to form semi-liquid droplets, is established as a target of selective autophagy. With Atg-PE, an autophagosome IM, placed on the outside of LUV and GUV membranes, it was observed that Ape1 droplets could be sequestered by membranes only when Atg19 receptor that binds Ape1 protein was present (Yamasaki et al., 2020) (Table 22.1, Fig. 22.2 – No. 11). Sufficient autophagic receptor concentration and cargo liquidity were both identified as determinants of condensates selective autophagy.

To reconstitute autophagosome biogenesis, the microtubule-associated protein 1 A/1B-light chain (LC3), which is a soluble protein, has been of primary interest. Cytosolic LC3 conjugation with phosphatidylethanolamine (PE) forms lipidated LC3 or LC3-PE/LC3-II that associates with autophagosomes. Artificial liposomes were used to reconstitute LC3 lipidation. On a GUV, PI(3)P was synthesized by PI3KC3-C1. The PI(3)P in turn recruited WIPI2 that promotes LC3 lipidation. Given the positive feedback loop that facilitated mutual recruitment of PI3KC3-C1 and WIPI2, this LC3 lipidation occurred rapidly, on par with cellular kinetics. The positive feedback loop in recruitment of PI3KC3-C1 and WIPI2 to LC3 lipidation was observed both in SUVs and in GUVs (Fracchiolla et al., 2020) (Table 22.1, Fig. 22.2 – No. 12). These efforts highlight the utility of membrane platforms not only in the context of the plasma membrane boundary, but also in revealing insight into morphogenesis and housekeeping of the intracellular organelles.

22.4 Movement: directed membrane deformation

Cytoplasmic filaments collectively called the cytoskeleton retain the structural integrity of the cell and regulate organization and movement of membrane and internal organelles. Cytoskeletal systems composed of microtubules (i.e., polymerized tubulin), intermediate filaments, septin, and actin cytoskeleton synergistically drive plasma membrane symmetry breaking that is the hallmark of adhesion-based directed cell motility, the primary focus of this section. Microtubules persist over long distances and modulate the global organization of the cell through MT-organizing centers, while actin cytoskeleton operates at the cell boundary and prompts rapid and local membrane dynamics.

22.4.1 Microtubules and motors

Tubulin heterodimer consists of α-tubulin that binds GTP and a β subunit that is a GTPase. Tubulin polymerizes to form microtubules (MTs) which are a rigid rod of 25 nm in diameter. This polymerization process is reversible and owing to its dynamic kinetics can regulate dynamic shape changes. MTs also interact with molecular motors such as dynein and kinesin to transport vesicles and proteins or to regulate motile apparati such as cilia, flagella, or muscle. Over the past decades actomyosin has taken the center spot as the main player of cell deformation. However, microtubules' role beyond housekeeping, in the realm of epithelial morphogenesis, is coming to light in more recent years (Röper, 2020).

MTs are sensitive to physical and chemical stimuli such as hydrostatic pressure, temperature, or small molecules, rendering them suitable inputs to trigger biochemical reactions *in vitro*. Cyclical application of hydrostatic pressure enabled modulation of MT polymerization reconstituted in GUVs. Importantly, reversible morphologies could also be achieved (Hayashi et al., 2016). To understand how centrally localized MTs can deform membranes, centrosome, tubulin, and GTP were reconstituted inside the GUVs whose membrane tension was modulated by controlling the external osmolarity of the vesicles. Depending on the tubulin concentration, asters of various lengths emerged and the ones surpassing the GUV diameter bent the membrane (Gavriljuk et al., 2021) (Table 22.1, Fig. 22.3 – No. 13).

To program molecular actuators, DNA complexed with kinesin was used to control (dis)assembly of the microtubules on demand. Cholesterol-modified DNA that can both be anchored to the membrane and transmit force were leveraged. A DNA strand displacement mechanism (termed "clutch") triggered translocation of the cytosolic microtubule and kinesin toward the membrane upon UV irradiation. Kinesin gliding on the MT in the proximity of the membrane induced dynamic membrane shape changes. Upon a further round of UV irradiation, the MT/kinesin proteins were released from the membrane, terminating the shape changing events (Sato et al., 2017) (Table 22.1, Fig. 22.3 – No. 14).

Self-propelled particles (SPP) that have a specific affinity for membranes were reconstituted in GUVs. As the SPPs encounter the membrane, they push it. A low-tension vesicle could be deformed with a single SPP. Due to cooperativity, a few SPPs trapped locally recruited more SPPs to the site, generating forces that gave rise to membrane tethers (Vutukuri et al., 2020) (Table 22.1, Fig. 22.3 – No. 15). The SPPs are polar in both direction of motion and interparticle interaction, distinguishing them from microtubules that exhibit nematic order and polarity in their motion but not in their interaction. However, the shapes achieved by these SPPs resembled those observed as the output of kinesin motor walking on a microtubule track. In this study both the vesicle membrane tension and the oscillation dynamics of kinesin motion was tuned to achieve the active biomimetic, shape-changing material (Keber et al., 2014) (Table 22.1, Fig. 22.3 – No. 16). Interestingly, by encapsulating a whole organism, motile *Bacillus subtilis* PY79 bacteria, inside GUVs, similar membrane fluctuations in the form of relatively long membrane projections were observed (Takatori & Sahu, 2020).

22.4.2 Actin and myosin

On the eukaryotic cell's plasma membrane, several regulatory mechanisms including protein switches, allosteric regulation of signal transduction, and redundant signaling pathways are known to amplify asymmetries (Goryachev & Leda, 2017; Inoue & Meyer, 2008; Ma & Nussinov, 2009; Nussinov et al., 2020). To extract the key players of actin-induced symmetry breaking, *in vitro* reconstitution in reduced membrane-bound systems that lack the cellular complexity has provided insights (Van Der Gucht & Sykes, 2009). When actin, gelsolin (an actin filament nucleator that restricts actin filament length), and filamin (a filament crosslinking protein) were reconstituted in vesicles, they deformed the membrane. Like MT observations, the deformation extent in this case was also a function of the filament length (Cortese et al., 1989) (Table 22.1, Fig. 22.3 – No. 17).

While cell-sized vesicles placed in a mixture of actin and its polymerization regulators experienced F-actin exerted forces on their membrane (Liu et al., 2008; Simon et al., 2019),

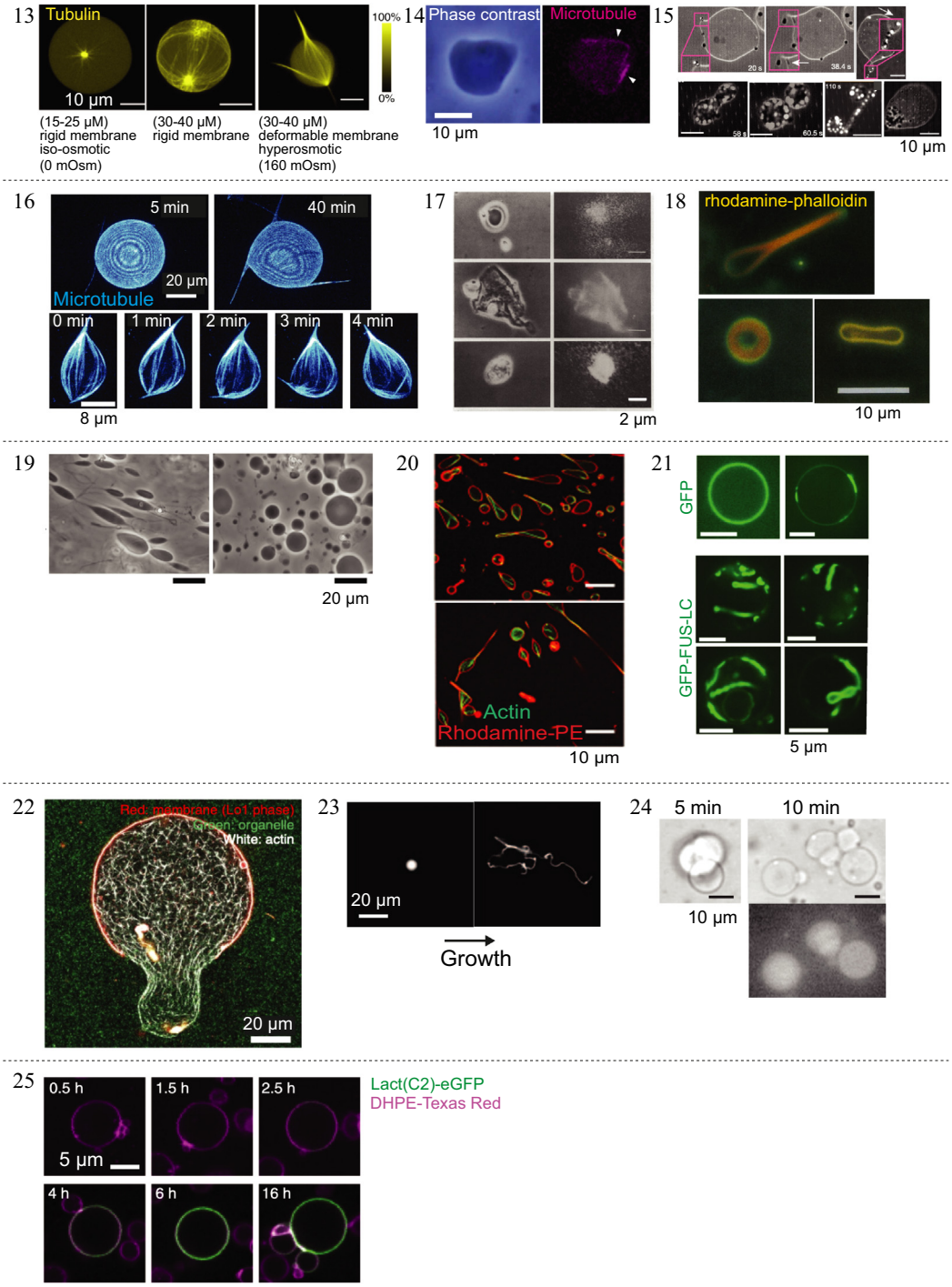

FIGURE 22.3 Representative images of the platforms presented in Table 22.1 (Nos. 13–25). Images are reprinted from the cited sources, either with permission of the respective copyright holders or under a Creative Commons license.

symmetry was broken only if either capping protein (CP) or myosin were present (Carvalho, Lemière, et al., 2013; Carvalho, Tsai, et al., 2013). Similar outputs were also featured using water-in-oil droplets surrounded by a monolayer of lipid either with the pure actomyosin network (Sakamoto et al., 2020) or ones supplemented with *Xenopus* egg extract (Ierushalmi et al., 2020; Malik-Garbi et al., 2019; Sakamoto et al., 2020). Of note, these experiments were carried out at an infinite source of biological materials and/or with these materials external to vesicles which is an opposite topology between biomolecules and membranes compared to physiological contexts. To better mimic a cell-like environment, engineering enclosed systems with autonomous actin-induced membrane polarity internal to vesicular membranes are of great interest. However, due to the lack of access to the inner content, they had to be coupled to an artificial external input. There were several ways to circumvent this. G-actin alone could polymerize and deform vesicles in response to elevated temperatures (Miyata & Hotani, 1992) (Table 22.1, Fig. 22.3 – No. 18) or addition of KCl via electroporated membranes (Miyata et al., 1999) resulted in similar outputs. A uniform actin cortex was formed upon delivery of ATP-containing polymerization buffer to the intravesicular space through membrane pores (Pontani et al., 2009). Alternatively, actin cortex was enriched by lowering the temperature of the emulsion phase replete with polymerization reaction and extracellular extracts (Abu Shah & Keren, 2014).

To drive motility, a sustained supply of actin is needed to retain the established front-back polarity observed in adherent cells. The actin turnover machinery facilitates this actin supply sustenance. With filamentous actin at concentrations comparable to that within cells, vesicles morphed into spindle shape without myosin. Light-irradiation of fluorescently labeled actin that severed actin polymers gave rise to a spherical morphology. It is not clear if the F-actin re-elongation is due to the spontaneous annealing or repolymerization (Tanaka et al., 2018) (Table 22.1, Fig. 22.3 – No. 19). Proteins that specifically bind actin filaments and crosslink them into bundles are α-actinin, fascin, and filamin. These crosslinkers modulate the stiffness of actin bundles and their membrane deformation propensity. By varying actin-fascin molar ratio it was observed that soft bundles output kinks and a web-like networks whereas stiff bundles remained straight in the main body (Tsai & Koenderink, 2015) (Table 22.1, Fig. 22.3 – No. 20). These underscore that a mode of regulation of cell shapes is directly achieved via changing the mechanical properties of the membranes.

More recently, actin rings, actin asters (Bashirzadeh et al., 2020, 2021) or Arp2/3-mediated dendritic actin cortex (Wubshet et al., 2021) were achieved inside GUVs in the presence of actin crosslinkers. Further, with either actin crosslinkers or actomyosin, contractile ring-like structures were achieved inside GUVs (Litschel et al., 2021). These bodies of work highlight that confining the vesicle geometry or anchoring actin to the membrane which both drive local enrichment of biomolecules are essential to achieving the drastic membrane protrusions observed.

22.5 Growth: biomaterial synthesis

To achieve cell-like function, construction of membrane-bound bioreactors that are energetically independent and could synthesize biomolecules such as lipids and oligonucleotides is under active study. For self-replication, growth of membrane precursors that can

extend the membrane, duplication of the genetic material, and its partitioning, all need to be realized. All these processes are also symmetry breaking events internal to a cell and consume energy in the form of ATP. Here, we first discuss protein phase separation as a minimal system to partition membranes. We then present several efforts on the construction of minimal membrane systems that can generate ATP, oligonucleotides, and lipids and further, could cyclically divide.

The impact of protein phase separation on membranes was studied using the fused in sarcoma low-complexity (FUS LC) protein domain that mediates liquid-liquid phase separation. FUS LC tagged with GFP was placed on the outside of giant vesicles made with plasma membrane of mammalian retinal pigmented epithelia (RPE) cells that express a nanobody against GFP. Protein phase separation on the membrane generated stresses that were large enough to drive an array of morphologies. These include inward protein-lined membrane buds, tubules with occasional pearling, and undulation that were achieved using giant plasma membrane vesicles (GPMV) derived from RPE cell membranes (Yuan et al., 2021) (Table 22.1, Fig. 22.3 – No. 21). Notably, it is speculated the energy barrier for assembly and disassembly of liquid scaffolds is lower than their protein counterparts. Therefore, the membranes associated with liquid scaffolds can have greater freedom to access a broader array of unique geometries (Yuan et al., 2021). Given the structural diversity of the organelles such as mitochondria and endoplasmic reticulum within cells, it is likely that cells use a combination of several deformation modes presented to sculpt themselves and carry out their functions.

ATP is the energy currency of the cell and therefore synthesizing its production could power autonomous cell-mimetic systems. To convert light to energy that drives mechanical work, a switchable photosynthetic organelle was achieved inside small vesicles that were in turn encapsulated in GUVs. ATP synthase and two distinct photoconverters reconstituted inside small vesicles drove the synthesis of ATP in the presence of light. This organelle-mimetic construction used the ATP to promote polymerization of actin and subsequently the deformation of the GUV membrane that housed it (Lee et al., 2018) (Table 22.1, Fig. 22.3 – No. 22). Moreover, photosynthetic cells were constructed by embedding GUVs with proteoliposomes containing two membrane proteins, bacteriorhodopsin and the F-type ATP synthase (F_0F_1). Upon 6 hours of light illumination about 1.8 mM ATP was generated inside a single vesicle. Once coupled with the IVTT system reconstituted inside the same GUVs, the photosynthesized ATP could drive both the mRNA transcription and protein translation. This enabled a positive feedback topology where the ATP could be consumed to synthesize the ATP-generation protein machinery, moving toward energy-independent synthetic cells (Berhanu et al., 2019).

To achieve cyclic growth and division of artificial cells, generation of lipids coupled to the amplification of genetic material must be realized. To this end, oleate micelles were added to monodisperse multilamellar oleate vesicles encapsulated with fluorescently-tagged RNA. A tail started to grow on the otherwise spherical vesicles and morphed into a long thread-like structure. Once exposed to shear forces exerted by blowing of compressed air, the thread divided into smaller spherical daughter vesicles, a process that could be cyclically implemented (Zhu & Szostak, 2009) (Table 22.1, Fig. 22.3 – No. 23). To integrate this system with both (1) an autonomous shear inducing, and (2) a gene amplifying mechanism, thermally stable GUVs with bolaamphiphilic lipids encapsulated with the polymerase chain reaction (PCR) were fabricated.

Bolaamphiphilic membrane precursors have hydrophilic groups on both ends, are cationic, and can insert themselves within the vesicle membrane (Fuhrhop & Wang, 2004). PCR-amplified DNA adhered to these membrane precursors in the inner leaflet of the GUV membrane, promoting division (Kurihara et al., 2011) (Table 22.1, Fig. 22.3 – No. 24).

To engineer a system that can synthesize the lipid precursors themselves, DNA-encoded phospholipid synthesis was realized. The 7 enzymes in the *E. coli* phospholipid synthesis pathway encoded in an individual transcriptional cassette were translated in GUVs using the IVTT system. Selective synthesis of six different lipid species was achieved. However, the concentration produced was not high enough to achieve visible membrane expansion, most likely stemming from the production rate of the IVTT system or the concentration of the enzyme precursors (Blanken et al., 2020) (Table 22.1, Fig. 22.3 – No. 25). For *de novo* synthesis of phospholipids, a soluble mycobacterial ligase was expressed from its DNA template using the IVTT system. In the lipid synthetic pathway selected, FadD10 formed fatty acyl adenylates that reacted with amine-functionalized lysolipids and formed phospholipids. This phospholipid assembled in the form of vesicles that could be detected with a confocal microscope. Notably these vesicles could further grow in size over time (Bhattacharya et al., 2019), capturing a key feature of a self-sustaining synthetic cell.

22.6 Challenges and future outlook

Reconstitution platforms with minimal biomolecular regulators have revealed much about the underlying biology. However, depending on the context, oversimplification can lead to artifactual interpretations. For instance, biological membranes are rich with membrane proteins that could be glycosylated, affecting the membrane property, the crowding landscape, and the reaction kinetics. Posttranslational modification status of purified proteins may differ depending on animal species where the proteins are harvested. Moreover, for most reconstitution efforts, buffer compositions are tailored to achieve a reaction and not necessarily mimic the cytosolic milieu (IVTT components are more representative of cytosol, even though they are at dilute regimes). Such considerations could resolve the disconnect between reconstitution efforts and cell-based assays that are more complex and feature faster kinetics.

While membrane platforms are paving the path toward more complex artificial systems, streamlining the bio-assembly process remains a roadblock. Contrary to DNA modules, lipids and proteins cannot be easily synthesized nor can they readily be cascaded to form a network of sequential reactions, hampering reconstitution efforts. Moreover, feasibility of fabrication of vesicular membranes given a prescribed lipid, protein, and buffer combination is not guaranteed. This is mainly due to considerations with lipid geometry, fluidity, biomolecular charges, ambient condition, and the fabrication method of choice (Razavi et al., 2021). On par with this consideration, translating the biological insight from a 2D space to a 3D one is not always straightforward. In many cases, given a vesicle fabrication technique, the lipid composition and protein concentrations must be optimized concurrently, adversely affecting throughput and the ability to directly compare a single variable across experiments. Moreover, irrespective of the source of the reconstituted proteins, purified or synthesized via IVTT systems, their supply remains limited with no cell-like synthesis or turn-over machinery that can operate indefinitely.

While these all are challenges, they put forth opportunities to not only enhance the design of these platforms or engineer new ones, but also further guide biological studies in cells. A comprehensive repertoire of fabrication techniques and the lipid compositions that these methods could accommodate would benefit the community. Perhaps dedicated fabrication studies with large throughput can provide a large set of data to a machine learning pipeline that can extract the lipid features that enable liposome formation. Such deep learning approaches can reveal the experimental landscape available or allow preliminary *in silico* feasibility assessment prior to an experimental venture. Furthermore, owing to the clear assessment of the genotype-phenotype link in these platforms, they are well-suited for directed evolution studies to uncover lipid-protein binding domains or protein structures that were otherwise buried in a signaling pathway.

As presented here, symmetry breaking lies at the core of the processes that constitute life. These reconstitution endeavors focus on the physical boundary of a cell or its organelles and illuminate the intricate molecular events that orchestrate morphogenesis at different length-scales. The evolution of the shapes achieved captures both the beauty and the perplexing features of their natural cellular origins. The utility of these achievements is, however, beyond the mimicry of nature. The design principles learned could inspire new classes of soft, micron-sized robots that could be deployed in any cellular milieu for diagnostic and therapeutic applications. Therefore, the ramifications of reconstitution of symmetry breaking are as impactful as they are beautiful (Longo & Montévil, 2011).

Acknowledgments

We would like to thank Dr. Hideaki T. Matsubayashi for insightful comments, and Robert DeRose for proofreading the manuscript. This work was supported by discretionary funds to T.I., the National Institutes of Health (R01GM136858 and R01GM123130 to T.I.), and the National Science Foundation (000819255 to T.I.). Figure 1 was created with BioRender.com.

Appendix

AF	Alexa Fluor
AP180	clathrin coat assembly protein, also known as AP3
ATP	adenosine triphosphate
DGS-NTA(Ni)	1,2-dioleoyl-sn-glycero-3-[(N-(5-amino-1-carboxypentyl) iminodiacetic acid)succinyl] (nickel salt)
DHPE	1,2-dihexadecanoyl-sn-glycero-3-phosphoethanolamine, triethylammonium salt
DMPC	1,2-dimyristoyl-sn-glycero-3-phosphocholine
DOPC	1,2-dioleoyl-sn-glycero-3-phosphocholine
DOPE	1,2-dioleoyl-sn-glycero-3-phosphoethanolamine
DOPG	1,2-dioleoyl-sn-glycero-3-phosphocholine
DPPC	1,2-dipalmitoyl-sn-glycero-3-phosphocholine
DPPE	1,2-Dipalmitoyl-sn-glycero-3-phosphoethanolamine
DSPE	1,2-Distearoyl-sn-glycero-3-phosphoethanolamine
ER	endoplasmic reticulum
ESCRT	endosomal sorting complexes required for transport
GPMV	giant plasma membrane vesicles
GUV	giant unilamellar vesicles
iLID	improved light-induced dimer module

IVTT	in vitro transcription-translation
LLPS	liquid-liquid phase separation
LUV	large unilamellar vesicles
MT	microtubule
PE	phosphatidylethanolamine
PL	L-α-phosphatidylinositol
PIP_2	PI(4,5)P_2 or Phosphatidylinositol 4,5-bisphosphate
POPC	1-palmitoyl-2-oleoyl-sn-glycero-3-phosphocholine
POPG	1-Palmitoyl-2-oleoyl-sn-glycero-3-(phospho-rac-(1-glycerol))
POPS	1-palmitoyl-2-oleoyl-sn-glycero-3-phospho-L-serine
PR	bacteria derived proteorhodopsin
PSII	plant-derived photosystem II (PSII)
PtdIns3*P*	phosphatidylinositol-3-phosphate
SLB	supported lipid bilayer
SPP	signal peptide peptidase
SUPER	supported bilayer with excess membrane reservoir
SUV	small unilamellar vesicles
TMR	tetra-methyl rhodamine
TXTL	cell-free transcription-translation

References

Abu Shah, E., & Keren, K. (2014). Symmetry breaking in reconstituted actin cortices. *eLife*, *3*, e01433–e01433.

Bashirzadeh, Y., Redford, S. A., Lorpaiboon, C., Groaz, A., Moghimianavval, H., Litschel, T., Schwille, P., Hocky, G. M., Dinner, A. R., & Liu, A. P. (2021). Actin crosslinker competition and sorting drive emergent GUV size-dependent actin network architecture. *Communications Biology*, *4*, 1136.

Bashirzadeh, Y., Wubshet, N. H., & Liu, A. P. (2020). Confinement geometry tunes fascin-actin bundle structures and consequently the shape of a lipid bilayer vesicle. *Frontiers in Molecular Biosciences*, *7*, 610277.

Berhanu, S., Ueda, T., & Kuruma, Y. (2019). Artificial photosynthetic cell producing energy for protein synthesis. *Nature Communications*, *10*, 1325.

Bhattacharya, A., Brea, R. J., Niederholtmeyer, H., & Devaraj, N. K. (2019). A minimal biochemical route toward de novo formation of synthetic phospholipid membranes. *Nature Communications*, *10*, 300.

Blanken, D., Foschepoth, D., Serrão, A. C., & Danelon, C. (2020). Genetically controlled membrane synthesis in liposomes. *Nature Communications*, *11*, 4317.

Cabré, E. J., Monterroso, B., Alfonso, C., Sánchez-Gorostiaga, A., Reija, B., Jiménez, M., Vicente, M., Zorrilla, S., & Rivas, G. (2015). The nucleoid occlusion SlmA protein accelerates the disassembly of the FtsZ protein polymers without affecting their GTPase activity. *PLoS One*, *10*, e0126434.

Carvalho, K., Lemière, J., Faqir, F., Manzi, J., Blanchoin, L., Plastino, J., Betz, T., & Sykes, C. (2013a). Actin polymerization or myosin contraction: two ways to build up cortical tension for symmetry breaking. *Philosophical Transactions of the Royal Society B: Biological Sciences*, *368*, 20130005.

Carvalho, K., Tsai, F.-C., Lees, E., Voituriez, R., Koenderink Gijsje, H., & Sykes, C. (2013b). Cell-sized liposomes reveal how actomyosin cortical tension drives shape change. *Proceedings of the National Academy of Sciences*, *110*, 16456–16461.

Cortese, J. D., Schwab, B., Frieden, C., & Elson, E. L. (1989). Actin polymerization induces a shape change in actin-containing vesicles. *Proceedings of the National Academy of Sciences*, *86*, 5773–5777.

Daley, D. O., Skoglund, U., & Söderström, B. (2016). FtsZ does not initiate membrane constriction at the onset of division. *Scientific Reports*, *6*, 33138.

Drake, M. T., Downs, M. A., & Traub, L. M. (2000). Epsin binds to clathrin by associating directly with the clathrin-terminal domain. Evidence for cooperative binding through two discrete sites. *Journal of Biological Chemistry*, *275*, 6479–6489.

Fracchiolla, D., Chang, C., Hurley, J. H., & Martens, S. (2020). A PI3K-WIPI2 positive feedback loop allosterically activates LC3 lipidation in autophagy. *Journal of Cell Biology*, 219.

Fuhrhop, J.-H., & Wang, T. (2004). Bolaamphiphiles. *Chemical Reviews*, *104*, 2901–2938.

Furusato, T., Horie, F., Matsubayashi, H. T., Amikura, K., Kuruma, Y., & Ueda, T. (2018). De novo synthesis of basal bacterial cell division proteins FtsZ, FtsA, and ZipA inside giant vesicles. *ACS Synthetic Biology*, *7*, 953–961.
Garenne, D., Libchaber, A., & Noireaux, V. (2020). Membrane molecular crowding enhances MreB polymerization to shape synthetic cells from spheres to rods. *Proceedings of the National Academy of Sciences of the United States of America*, *117*, 1902–1909.
Gavriljuk, K., Scocozza, B., Ghasemalizadeh, F., Seidel, H., Nandan, A. P., Campos-Medina, M., Schmick, M., Koseska, A., & Bastiaens, P. I. H. (2021). A self-organized synthetic morphogenic liposome responds with shape changes to local light cues. *Nature Communications*, *12*, 1548.
Godino, E., López, J. N., Zarguit, I., Doerr, A., Jimenez, M., Rivas, G., & Danelon, C. (2020). Cell-free biogenesis of bacterial division proto-rings that can constrict liposomes. *Communications Biology*, *3*, 539.
Goryachev, A. B., & Leda, M. (2017). Many roads to symmetry breaking: molecular mechanisms and theoretical models of yeast cell polarity. *Molecular Biology of the Cell*, *28*, 370–380.
Hayashi, M., Nishiyama, M., Kazayama, Y., Toyota, T., Harada, Y., & Takiguchi, K. (2016). Reversible morphological control of tubulin-encapsulating giant liposomes by hydrostatic pressure. *Langmuir*, *32*, 3794–3802.
Helfrich, W. (1973). Elastic properties of lipid bilayers: theory and possible experiments. *Zeitschrift für Naturforschung C*, *28*, 693–703.
Ierushalmi, N., Malik-Garbi, M., Manhart, A., Abu Shah, E., Goode, B. L., Mogilner, A., & Keren, K. (2020). Centering and symmetry breaking in confined contracting actomyosin networks. *Elife*, *9*.
Inoue, T., & Meyer, T. (2008). Synthetic activation of endogenous PI3K and Rac identifies an AND-gate switch for cell polarization and migration. *PLoS One*, *3*, e3068.
Keber, F. C., Loiseau, E., Sanchez, T., Decamp, S. J., Giomi, L., Bowick, M. J., Marchetti, M. C., Dogic, Z., & Bausch, A. R. (2014). Topology and dynamics of active nematic vesicles. *Science*, *345*, 1135–1139.
Kurihara, K., Tamura, M., Shohda, K., Toyota, T., Suzuki, K., & Sugawara, T. (2011). Self-reproduction of supramolecular giant vesicles combined with the amplification of encapsulated DNA. *Nat Chem*, *3*, 775–781.
Lee, K. Y., Park, S.-J., Lee, K. A., Kim, S.-H., Kim, H., Meroz, Y., Mahadevan, L., Jung, K.-H., Ahn, T. K., Parker, K. K., & Shin, K. (2018). Photosynthetic artificial organelles sustain and control ATP-dependent reactions in a protocellular system. *Nature Biotechnology*, *36*, 530–535.
Litschel, T., Kelley, C. F., Holz, D., Adeli Koudehi, M., Vogel, S. K., Burbaum, L., Mizuno, N., Vavylonis, D., & Schwille, P. (2021). Reconstitution of contractile actomyosin rings in vesicles. *Nature Communications*, *12*, 2254.
Litschel, T., Ramm, B., Maas, R., Heymann, M., & Schwille, P. (2018). Beating vesicles: encapsulated protein oscillations cause dynamic membrane deformations. *Angewandte Chemie International Edition*, *57*, 16286–16290.
Liu, A. P., Richmond, D. L., Maibaum, L., Pronk, S., Geissler, P. L., & Fletcher, D. A. (2008). Membrane-induced bundling of actin filaments. *Nature Physics*, *4*, 789–793.
Longo, G., & Montévil, M. (2011). From physics to biology by extending criticality and symmetry breakings. *Progress in Biophysics and Molecular Biology*, *106*, 340–347.
Loose, M., Fischer-Friedrich, E., Ries, J., Kruse, K., & Schwille, P. (2008). Spatial regulators for bacterial cell division self-organize into surface waves in vitro. *Science*, *320*, 789–792.
Ma, B., & Nussinov, R. (2009). Amplification of signaling via cellular allosteric relay and protein disorder. *Proceedings of the National Academy of Sciences of the United States of America*, *106*, 6887–6888.
Maeda, Y. T., Nakadai, T., Shin, J., Uryu, K., Noireaux, V., & Libchaber, A. (2012). Assembly of MreB filaments on liposome membranes: a synthetic biology approach. *ACS Synthetic Biology*, *1*, 53–59.
Malik-Garbi, M., Ierushalmi, N., Jansen, S., Abu-Shah, E., Goode, B. L., Mogilner, A., & Keren, K. (2019). Scaling behaviour in steady-state contracting actomyosin networks. *Nature Physics*, *15*, 509–516.
Meier, E. L., Razavi, S., Inoue, T., & Goley, E. D. (2016). A novel membrane anchor for FtsZ is linked to cell wall hydrolysis in *Caulobacter crescentus*. *Molecular Microbiology*, *101*, 265–280.
Miyata, H., & Hotani, H. (1992). Morphological changes in liposomes caused by polymerization of encapsulated actin and spontaneous formation of actin bundles. *Proceedings of the National Academy of Sciences of the United States of America*, *89*, 11547–11551.
Miyata, H., Nishiyama, S., Akashi, K., & Kinosita, K., JR. (1999). Protrusive growth from giant liposomes driven by actin polymerization. *Proceedings of the National Academy of Sciences of the United States of America*, *96*, 2048–2053.
Monterroso, B., Zorrilla, S., Sobrinos-Sanguino, M., Robles-Ramos Miguel, Á., Alfonso, C., Söderström, B., Meiresonne Nils, Y., Verheul, J., Den Blaauwen, T., Rivas, G., & Brennan Richard, G. (2019). The bacterial

DNA binding protein MatP involved in linking the nucleoid terminal domain to the divisome at midcell interacts with lipid membranes. *mBio*, *10*, e00376-19.
Morlot, S., & Roux, A. (2013). Mechanics of dynamin-mediated membrane fission. *Annual Review of Biophysics*, *42*, 629–649.
Nussinov, R., Tsai, C. J., & Jang, H. (2020). Are parallel proliferation pathways redundant? *Trends in Biochemical Sciences*, *45*, 554–563.
Osawa, M., & Erickson, H. P. (2013). Liposome division by a simple bacterial division machinery. *Proceedings of the National Academy of Sciences of the United States of America*, *110*, 11000–11004.
Osawa, M., Anderson, D. E., & Erickson, H. P. (2008). Reconstitution of contractile FtsZ rings in liposomes. *Science*, *320*, 792–794.
Pfitzner, A. K., Mercier, V., Jiang, X., Moser Von Filseck, J., Baum, B., Šarić, A., & Roux, A. (2020). An ESCRT-III polymerization sequence drives membrane deformation and fission. *Cell*, *182*, 1140–1155, e18.
Pontani, L.-L., Van Der Gucht, J., Salbreux, G., Heuvingh, J., Joanny, J.-F., & Sykes, C. (2009). Reconstitution of an actin cortex inside a liposome. *Biophysical Journal*, *96*, 192–198.
Pucadyil, T. J., & Schmid, S. L. (2008). Real-time visualization of dynamin-catalyzed membrane fission and vesicle release. *Cell*, *135*, 1263–1275.
Ramirez-Diaz, D. A., Merino-Salomón, A., Meyer, F., Heymann, M., Rivas, G., Bramkamp, M., & Schwille, P. (2021). FtsZ induces membrane deformations via torsional stress upon GTP hydrolysis. *Nature Communications*, *12*, 3310.
Ramm, B., Goychuk, A., Khmelinskaia, A., Blumhardt, P., Eto, H., Ganzinger, K. A., Frey, E., & Schwille, P. (2021). A diffusiophoretic mechanism for ATP-driven transport without motor proteins. *Nature Physics*, *17*, 850–858.
Razavi, S., Inoue, T., Tianzhi, L., & Robinson, D., 2021. Methods for making giant vesicles and their use. Google Patents.
Röper, K. (2020). Microtubules enter centre stage for morphogenesis. *Philosophical Transactions of the Royal Society B: Biological Sciences*, *375*, 20190557.
Sakamoto, R., Tanabe, M., Hiraiwa, T., Suzuki, K., Ishiwata, S., Maeda, Y. T., & Miyazaki, M. (2020). Tug-of-war between actomyosin-driven antagonistic forces determines the positioning symmetry in cell-sized confinement. *Nature Communications*, *11*, 3063.
Saleem, M., Morlot, S., Hohendahl, A., Manzi, J., Lenz, M., & Roux, A. (2015). A balance between membrane elasticity and polymerization energy sets the shape of spherical clathrin coats. *Nature Communications*, *6*, 6249.
Sato, Y., Hiratsuka, Y., Kawamata, I., Murata, S., & Nomura, S. M. (2017). Micrometer-sized molecular robot changes its shape in response to signal molecules. *Science Robotics*, 2.
Schöneberg, J., Pavlin, M. R., Yan, S., Righini, M., Lee, I. H., Carlson, L. A., Bahrami, A. H., Goldman, D. H., Ren, X., Hummer, G., Bustamante, C., & Hurley, J. H. (2018). ATP-dependent force generation and membrane scission by ESCRT-III and Vps4. *Science*, *362*, 1423–1428.
Simon, C., Kusters, R., Caorsi, V., Allard, A., Abou-Ghali, M., Manzi, J., Di Cicco, A., Lévy, D., Lenz, M., Joanny, J.-F., Campillo, C., Plastino, J., Sens, P., & Sykes, C. (2019). Actin dynamics drive cell-like membrane deformation. *Nature Physics*, *15*, 602–609.
Snead, W. T., Hayden, C. C., Gadok, A. K., Zhao, C., Lafer, E. M., Rangamani, P., & Stachowiak, J. C. (2017). Membrane fission by protein crowding. *Proceedings of the National Academy of Sciences of the United States of America*, *114*, E3258-e3267.
Söderström, B., Skoog, K., Blom, H., Weiss, D. S., Von Heijne, G., & Daley, D. O. (2014). Disassembly of the divisome in *Escherichia coli*: evidence that FtsZ dissociates before compartmentalization. *Molecular Microbiology*, *92*, 1–9.
Stachowiak Jeanne, C., Hayden Carl, C., & Sasaki Darryl, Y. (2010). Steric confinement of proteins on lipid membranes can drive curvature and tubulation. *Proceedings of the National Academy of Sciences*, *107*, 7781–7786.
Stachowiak, J. C., Schmid, E. M., Ryan, C. J., Ann, H. S., Sasaki, D. Y., Sherman, M. B., Geissler, P. L., Fletcher, D. A., & Hayden, C. C. (2012). Membrane bending by protein-protein crowding. *Nature Cell Biology*, *14*, 944–949.
Steinkühler, J., Knorr, R. L., Zhao, Z., Bhatia, T., Bartelt, S. M., Wegner, S., Dimova, R., & Lipowsky, R. (2020). Controlled division of cell-sized vesicles by low densities of membrane-bound proteins. *Nature Communications*, *11*, 905.
Takatori, S. C., & Sahu, A. (2020). Active contact forces drive nonequilibrium fluctuations in membrane vesicles. *Physical Review Letters*, *124*, 158102.

Tanaka, S., Takiguchi, K., & Hayashi, M. (2018). Repetitive stretching of giant liposomes utilizing the nematic alignment of confined actin. *Communications Physics*, *1*, 18.

Tsai, F.-C., & Koenderink, G. H. (2015). Shape control of lipid bilayer membranes by confined actin bundles. *Soft Matter*, *11*, 8834–8847.

Van Der Gucht, J., & Sykes, C. (2009). Physical model of cellular symmetry breaking. *Cold Spring Harbor Perspectives in Biology*, *1*, a001909.

Vutukuri, H. R., Hoore, M., Abaurrea-Velasco, C., Van Buren, L., Dutto, A., Auth, T., Fedosov, D. A., Gompper, G., & Vermant, J. (2020). Active particles induce large shape deformations in giant lipid vesicles. *Nature*, *586*, 52–56.

Weyl, H. (1952). *Symmetry*. Princeton University Press.

Wollert, T., Wunder, C., Lippincott-Schwartz, J., & Hurley, J. H. (2009). Membrane scission by the ESCRT-III complex. *Nature*, *458*, 172–177.

Wubshet, N. H., Bashirzadeh, Y., & Liu, A. P. (2021). Fascin-induced actin protrusions are suppressed by dendritic networks in giant unilamellar vesicles. *Molecular Biology of the Cell*, *32*, 1634–1640.

Yamasaki, A., Alam, J. M., Noshiro, D., Hirata, E., Fujioka, Y., Suzuki, K., Ohsumi, Y., & Noda, N. N. (2020). Liquidity is a critical determinant for selective autophagy of protein condensates. *Molecular Cell*, *77*, 1163–1175, e9.

Yuan, F., Alimohamadi, H., Bakka, B., Trementozzi, A. N., Day, K. J., Fawzi, N. L., Rangamani, P., & Stachowiak, J. C. (2021). Membrane bending by protein phase separation. *Proceedings of the National Academy of Sciences of the United States of America*, *118*.

Zhu, T. F., & Szostak, J. W. (2009). Coupled growth and division of model protocell membranes. *Journal of the American Chemical Society*, *131*, 5705–5713.